Materials of the Future: Smart Applications in Science and Engineering _2021 E-conference, Center for Advanced Materials (CAM) and Biomedical Research Center (BRC), Qatar University, Qatar , March 29-31 (2021).

CFD simulation of Diamond and Zinc Smart Nanoparticles Performance in a Water-Based Trapezium Direct Absorber Solar Collector

Sireetorn Kuharat[1], O. Anwar Bég[1], Ali Kadir[1] and W.S.Jouri[1]
[1]Department of Mechanical/Aeronautical Engineering, Salford University, Manchester, M54WT, UK.
Presenting Author Email: s.kuharat@edu.salford.ac.uk

1.INTRODUCTION

In recent years, many nanomaterials have been deployed in solar energy systems. These include both carbon-based and metallic nanoparticles. By combining these nanoparticles with water base fluids, to create nanofluids, improved performance can be achieved in direct absorber solar collector (DASC) systems. In the current work, motivated by these developments, a finite volume code (ANSYS FLUENT) is employed to simulate the relative performance of both carbon-based (diamond) and metal-based (zinc) nanoparticles in a trapezium geometry. The Tiwari-Das formulation is implemented to compute viscosity, thermal conductivity and heat capacity properties for diamond-water and zinc-water nanofluids at different volume fractions. Steady state nanofluid buoyancy-driven incompressible laminar Newtonian convection is examined. The SIMPLE solver is deployed, and residual iterations utilized for convergence monitoring. Mesh independence is included. Verification with the penalty finite element computations of (Natarajan et al.) [1] for the case of a Newtonian viscous fluid (zero volume fraction) is also conducted and excellent correlation achieved. Isotherm, streamline and local Nusselt number plots are presented for different volume fractions, sloping wall inclinations (both negative and positive slopes are considered) and Rayleigh numbers. Vortex structure and thermal distributions are shown to be modified considerably with these parameters. Overall diamond achieves higher heat transfer rates while more stable velocity distributions are produced with zinc nanoparticles. These trends are amplified at higher volume fractions. The present computations may be further generalized to the three-dimensional case although this requires significantly greater mesh densities and compilation times.

2. MATHEMATICAL MODEL AND GEOMETRIC MESH

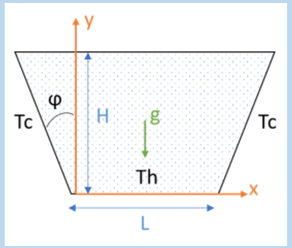

Figure 1: Trapezium water nanofluid direct absorber solar collector

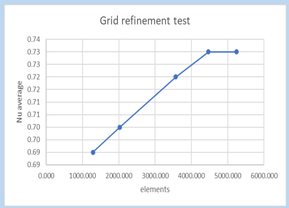

Figure 2: Grid refinement test

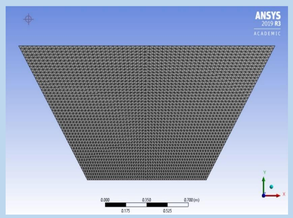

Figure 3: Final Mesh design for nanofluid DASC

The simulated 2-D geometry and boundary condition is shown in Fig. ANSYS FLUENT uses the finite-volume method to solve the governing Navier-Stokes equations for a fluid which are derived from the conservation mass equation (1), the conservation of momentum (2, 3) and Energy equation (4) for the following boundary conditions (5).

Continuity Equation:

$$\frac{\partial u}{\partial x}+\frac{\partial v}{\partial y}=0 \qquad (1)$$

x-direction momentum

$$u\frac{\partial u}{\partial x}+v\frac{\partial u}{\partial y}=-\frac{1}{\rho}\frac{\partial p}{\partial x}+\nu\nabla^2 u \qquad (2)$$

y-direction momentum

$$u\frac{\partial v}{\partial x}+v\frac{\partial v}{\partial y}=-\frac{1}{\rho}\frac{\partial p}{\partial y}+\nu\nabla^2 v+g\beta(T-T_c) \qquad (3)$$

Energy equation

$$u\frac{\partial T}{\partial x}+v\frac{\partial T}{\partial y}=\frac{k_{nf}}{\rho_{nf}c_p}\nabla^2 T \qquad (4)$$

Left cold wall: Constant temperature, T= 300 K

Right cold wall: Constant temperature, T= 300 K

Bottom hot wall: Constant temperature, T= 305 K (5)

The remaining walls: Adiabatic

The Tiwari-Das formulation [2] is implemented to compute viscosity, thermal conductivity and heat capacity properties for diamond-water and zinc-water nanofluids at different volume fractions:

The nano-particle volume fraction: $\phi=\frac{v_{np}}{vf}$ (6)

The nanofluid dynamic viscosity: $\mu_{nf}=\frac{\mu f}{(1-\phi)^{2.5}}$ (7)

The nanofluid density: $\rho_{nf}=(1-\phi)\rho f+\phi\rho s$ (8)

The nanofluid heat capacity: $Cp_{nf}=\frac{(1-\phi)(\rho Cp)_f+\phi(\rho Cp)_s}{\rho_{nf}}$ (9)

The thermal conductivity: $\frac{Knf}{kf}=\frac{ks+2kf-2\phi(kf-ks)}{ks+2kf-\phi(kf-ks)}$ (10)

Here k_{nf}=nanofluid thermal conductivity, k_f= fluid thermal conductivity and k_s= nanoparticle thermal conductivity.

Extensive grid independence tests were conducted of the trapezium mesh for trapezium geometry with ϕ=30 and Ra 105 shown in Figure 2 within the grid dependent study five different uniform grids system of 1288, 2030, 3572, 4472 and 5244 are conducted. The result in an average Nusselt number of the fluid is increase with a number of the elements until a small difference is observed between 4472 elements and 5244 elements which can be consider negligible which indicated that the simulation is convergent. The finalized mesh is shown in Figure 3 5244 triangular elements were deployed

3. ANSYS CFD VALIDATION

To verify the accuracy of the ANSYS FLUENT computations, a comparison has also been made for the purely Newtonian fluid case with the exact trapezium geometry and boundary conditions employed in the finite element simulations of (Natarajan, et al., 2008). The comaprison of temperature contours (isotherms) is shown in Figure 4.

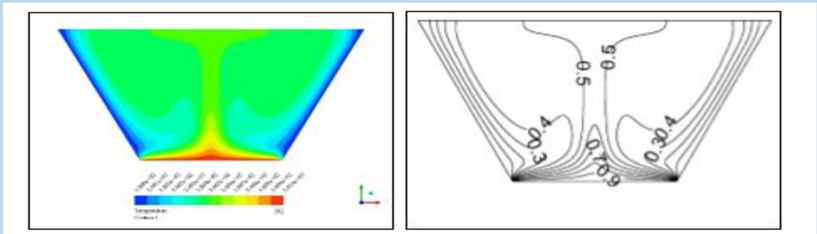

Figure 4: Comparison of ANSYS FLUENT and FEM solution of (Natarajan, et al., 2008) [1]

4. RESULTS AND DISCUSSION

Effects of Rayleigh number and inclination on the isotherms of water-based diamond nanofluid

The progression of flow and thermal fields within the trapezoidal enclosure for Ra = 103, 104, 105, and 106 and tilt angle, Ø = 20°, 10°, 0°, and -10° are presented in Figure 5-Figure 9. The flow and temperature fields are symmetrical about the vertical y-axis as boundary conditions are the same for both left and right inclined sidewalls. As predicted, hot fluid mainly rises up from the middle of the heated wall due to an effect of thermal buoyancy force. The flow is redirected down along the walls forming two symmetric vortex cells with clockwise and anticlockwise rotations inside the cavity. With increasing Rayleigh number, the hot zone at the trapezium base is progressively suppressed. Heat transfer to the wall is therefore inhibited. However, there is a concurrent expansion in warmer fluid through the core region and the cooler zones at the sidewalls are contracted. Heat is therefore circulated more efficiently in the enclosure with increasing thermal buoyancy effect.

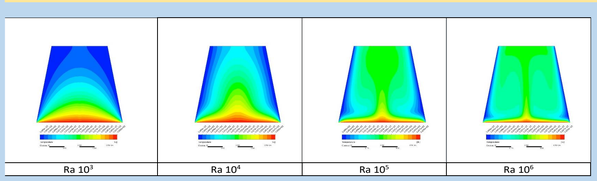

Figure 5: Diamond-Water Based Nanofluid with volume faction φ = 0.02, angle (Ø)=-10°

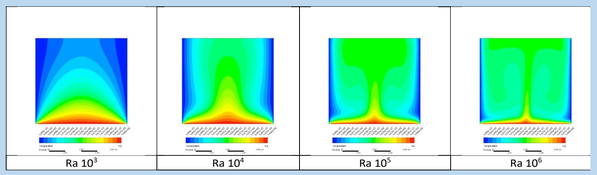

Figure 6: Diamond-Water Based Nanofluid with volume faction φ = 0.02, angle (Ø)=0°

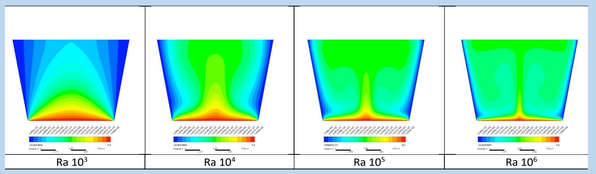

Figure 7: Diamond-Water Based Nanofluid with volume faction φ = 0.02, angle (Ø)=10°

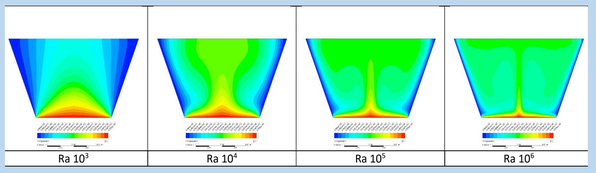

Figure 8: Diamond-Water Based Nanofluid with volume faction φ = 0.02, angle (Ø)=20°

At very high Rayleigh number (with volume fraction fixed at 2%, diamond nanofluid case, Figure 5) the streamlines are also morphed considerably, and the dual vortex structure is stretched in the vertical direction. The cells are increasingly lop-sided as compared with lower Rayleigh numbers. For the rectangular case (slope angle = 0) and the same volume fraction (2%, diamond case), the green zones are significantly expanded in the upper section of the enclosure with increasing Rayleigh number. Also, there is an elimination in the skewing of the dual vortex zones at higher Rayleigh numbers. however, some distortion is induced at the upper and lower wall zones in the streamlines which are not as controlled as in the trapezium case. With positive side wall inclination (10 degrees), as observed in

Figure 7, there is a much more consistent distribution of heat achieved throughout the trapezium and this is encouraged with greater Rayleigh number. However, at highest Rayleigh number, colder regions emerge in a symmetric fashion which implies that a critical Rayleigh number between 106 and 107 exists where the best temperature distribution is obtained in the solar collector.

The dual vortex structure witnessed in the streamlines is much more stable in Figure 7 than in previous figures (negative slop case, Figure 5 and rectangular case, Figure 6). This would indicate that the strong positive slope trapezium produces the most regulated circulation compared with the other configurations. However, it does not achieve the best heat transfer to the boundaries, which is generally obtained with the strong negative slope case (Figure 5 i.e., -10 degrees inclination). While the trend in isotherms is sustained with even greater positive sidewall slope (Figure 8) i.e., expansion in homogenous heat distribution, the vortex cells (streamlines) are increasingly warped with higher Rayleigh numbers, in particular at the top left and right corners of the cavity- see Kuharat [3].

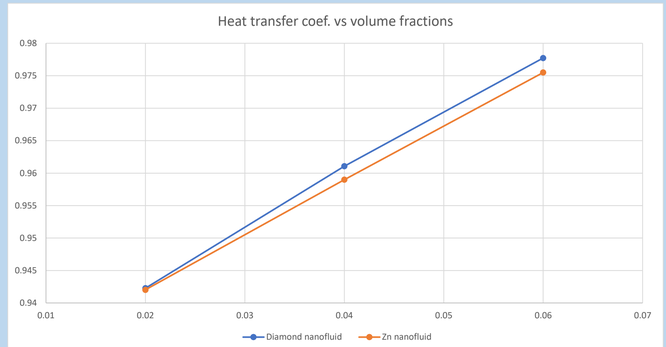

Figure 9 Heat transfer coef. vs volume fractions

Figure 9 depicts the variation in heat transfer coef. vs volume fractions for both diamond and zinc-water nanofluid. At low volume fraction (2%) both achieve approximately the same magnitude in heat transfer coefficient. However, with increasing volume fraction, the profiles diverge significantly and diamond-water nanofluid produces a markedly higher heat transfer coefficient which is maximum at the highest volume fraction of 6%.

5. CONCLUSIONS

A theoretical and numerical study of the relative performance of both carbon-based (i.e., diamond) and metal-based (i.e., zinc) water -nanofluids in a trapezoidal geometry has been presented. Steady state nanofluid buoyancy-driven incompressible laminar Newtonian convection is examined. A finite volume code (ANSYS FLUENT ver 19.1) is employed for the simulations with the SIMPLE solver, residual iterations utilized for convergence monitoring. Mesh independence is included. Verification with the penalty finite element computations of (Natarajan, et al., 2008)for the case of a Newtonian viscous fluid (zero volume fraction) is also conducted and excellent correlation achieved. Isotherm, streamline and local Nusselt number plots are presented for different volume fractions, sloping wall inclinations (both negative and positive slopes are considered) and Rayleigh numbers. The simulations have shown that:

i. **Diamond achieves higher heat transfer rates than zinc nanoparticles. Increasing heat transfer coefficients are computed with a rise in nanoparticle volume fraction for both diamond and zinc.**

ii. **Constant temperature sidewalls in the case of a strong negative slope (-10 degrees) act as heat sinks which move closer to the heat source resulting in improved heat transfer to the walls of the cavity.**

iii. **The strong positive slope trapezium case (inclination of +10 degrees) produces the most regulated circulation compared with the other configurations, although it does not achieve the best heat transfer to the boundaries – this is obtained with the strong negative slope case (i.e., -10 degrees inclination).**

iv. **For the rectangular case (slope angle = 0) in the diamond water nanofluid case, more homogeneous temperature distribution is achieved throughout the enclosure compared with any trapezium scenario and the skewing of the dual vortex zones at higher Rayleigh numbers is eliminated.**

v. **vii) For the strong positive slope trapezium case (+10 degrees inclination) compared with the strong negative slope trapezium case (-10 degrees inclination), at very high Rayleigh number (volume fraction 2%, diamond nanofluid case) The cells are increasingly lop-sided as compared with lower Rayleigh numbers for both sloped wall cases.**

vi. **The present computations have furnished some interesting insights into the relative performance of zinc and diamond water nanofluids in trapezium and rectangular solar enclosures.**

REFERENCES

[1] Natarajan, E., Basak, T. & Roy, S., 2008. Natural convection flows in a trapezoidal enclosure with uniform and non-uniform heating of bottom wall. *International Journal of Heat and Mass Transfer*, Volume 51, pp. 747-756 .

[2] Tiwari, R. K. & Das, M. K., 2007. Heat transfer augmentation in a two-sided lid-driven differentially heated square cavity utilizing nanofluids. *International Journal of Heat and Mass Transfer*, Volume 50, p. 2002–2018.

[3] S. Kuharat, Numerical study of nanofluid-based direct absorber solar collector systems with metallic/carbon nanoparticles, multiple geometries and multi-mode heat transfer, *PhD Thesis, Aerospace Engineering, University of Salford, Manchester, UK, March* (2021).